

# Nanowire-based single-cell endoscopy

Ruoxue Yan<sup>1†</sup>, Ji-Ho Park<sup>1,2†</sup>, Yeonho Choi<sup>3,4</sup>, Chul-Joon Heo<sup>3,5</sup>, Seung-Man Yang<sup>5</sup>, Luke P. Lee<sup>3</sup>  
and Peidong Yang<sup>1\*</sup>

**One-dimensional smart probes based on nanowires and nanotubes that can safely penetrate the plasma membrane and enter biological cells are potentially useful in high-resolution<sup>1–6</sup> and high-throughput<sup>7,8</sup> gene and drug delivery, biosensing<sup>6,9</sup> and single-cell electrophysiology<sup>6,10</sup>. However, using such probes for optical communication across the cellular membrane at the subwavelength level remains limited. Here, we show that a nanowire waveguide attached to the tapered tip of an optical fibre can guide visible light into intracellular compartments of a living mammalian cell, and can also detect optical signals from subcellular regions with high spatial resolution. Furthermore, we show that through light-activated mechanisms the endoscope can deliver payloads into cells with spatial and temporal specificity. Moreover, insertion of the endoscope into cells and illumination of the guided laser did not induce any significant toxicity in the cells.**

Optical nanoscopy, a high-resolution technique that breaks the diffraction barrier, has been introduced recently to study chemistry, biology and physics in intracellular molecular processes<sup>11–13</sup>. Although current optical techniques have now reached the subcellular level, high-precision optical imaging systems are complex, expensive and bulky. Therefore, incorporating a nanophotonic component into simple, low-cost, bench-top optical set-ups would miniaturize spectroscopic analyses, and would be particularly useful for studying chemical and biological events inside single cells as well as their substructures. Fluorescence sensing techniques based on submicrometre tapered optical fibres have been developed for probing living biological specimens<sup>14–17</sup>, but the requisite large and conical fibres mean that their illumination volume remains large and they can easily rupture cellular membranes. Nevertheless, fibre-optic fluorescence imaging techniques have unique features that can be incorporated into handheld optical systems and flexible endoscopes for minimally invasive imaging of opaque biological specimens such as tissues<sup>18</sup>. Integrating nanophotonic probes into the fibre-optic imaging system allows us to manipulate light at the nanoscale inside living cells for studying photoactive biological processes<sup>19,20</sup> and for bioanalytical analyses<sup>21,22</sup>.

Previously, we have shown that subwavelength dielectric nanowire waveguides can efficiently shuttle ultraviolet and visible light in air and fluidic media<sup>23,24</sup>. Nanowires are promising for interrogating intracellular environments, because their small dimensions (~100–250 nm) and mechanical flexibility minimize the damage they inflict on cellular structures and functions. Furthermore, because of their higher refractive index ( $n \approx 2.1$ – $2.2$ ) than that of conventional optical fibre ( $n \approx 1.5$ ), the nanowires can guide visible light efficiently in high-index physiological liquids and living cells ( $n \approx 1.3$ – $1.5$ ). In addition, the oxide surface of nanowires can be functionalized readily, enabling payload delivery and specific

sensing inside cells. Recently, there have been an increasing number of efforts to interface nanowire arrays with living cells to modulate the physicochemical properties of the cells and deliver biomolecules into subcellular environments<sup>25–27</sup>. By controlling nanowire diameter, length and density, they can be safely internalized into the cell without disturbing cell proliferation and differentiation.

Here, by combining the advantages of nanowire waveguides and a fibre-optic fluorescence imaging technique, we have designed a novel nanowire-based endoscope system (Fig. 1a) for optical probing inside single cells and the spatiotemporal delivery of payloads into intracellular sites with minimal perturbation to the cellular system.

The nanowire endoscope was fabricated by bonding a SnO<sub>2</sub> nanowire to the tapered tip of an optical fibre (Supplementary Fig. S1,S2). Light travelling along the optical fibre can be effectively coupled into the nanowire and travel to the nanowire tip, where it is re-emitted to free space (Fig. 1b). Mechanical stability is a fundamental requirement for biological probes for use in intracellular sensing and imaging. The nanowire endoscope is extremely flexible due to its small size and high aspect ratio, yet it is mechanically robust, and can endure repeated deformation, bending and buckling cycles without being peeled off the fibre. Figure 1d shows that, under 20° deformation, the nanowire remained firmly attached to the fibre tip. Also, the intensity of its tip emission did not show a significant fall-off compared to that when it was free of mechanical deformation (Fig. 1c), indicating that the optical coupling also remained undisturbed.

Highly efficient optical coupling between the nanowire and the optical fibre is crucial for nanowire endoscopes to function as localized light sources. To test the waveguiding capability of the nanowire endoscope in a physiological environment and to visualize the intensity distribution of the endoscope emission, the endoscope was immersed in cell culture media, which contains fluorescent proteins that can be excited by the endoscope (Fig. 1e). The profile of fluorescence intensity follows that of the endoscope emission (Fig. 1f,g). For a highly efficient nanowire endoscope, the optical output is closely confined to the nanowire tip, offering highly directional and localized illumination. Despite the small dimensions of the nanowires, the large increase (~33%) in environmental refractive index did not affect the optical coupling or light propagation, benefiting from the high refractive index of the SnO<sub>2</sub>.

The advantage of using nanowires instead of tapered fibre-optics for single-cell endoscopy is that nanowires are less invasive because of their fine diameters and uniform geometry. As in previous studies on silicon and gallium phosphide nanowire arrays<sup>25–27</sup>, where the nanowires were found to penetrate the lipid membrane of cells without causing any damage to cellular functions, the insertion of our SnO<sub>2</sub> nanowire into the cell cytoplasm did not induce cell

<sup>1</sup>Department of Chemistry, University of California, and Materials Sciences Division, Lawrence Berkeley National Laboratory, Berkeley, California 94720, USA, <sup>2</sup>Department of Bio and Brain Engineering, Korea Advanced Institute of Science and Technology, Daejeon 305-701, South Korea, <sup>3</sup>Department of Bioengineering, University of California, Berkeley, California 94720, USA, <sup>4</sup>Department of Biomedical Engineering, Korea University, Seoul, 136-703, South Korea, <sup>5</sup>CRI Center for Integrated Optofluidic Systems, Department of Chemical and Biomolecular Engineering, Korea Advanced Institute of Science and Technology, Daejeon, 305-701, South Korea. †These authors contributed equally to this work. \*e-mail: p\_yang@uclink.berkeley.edu

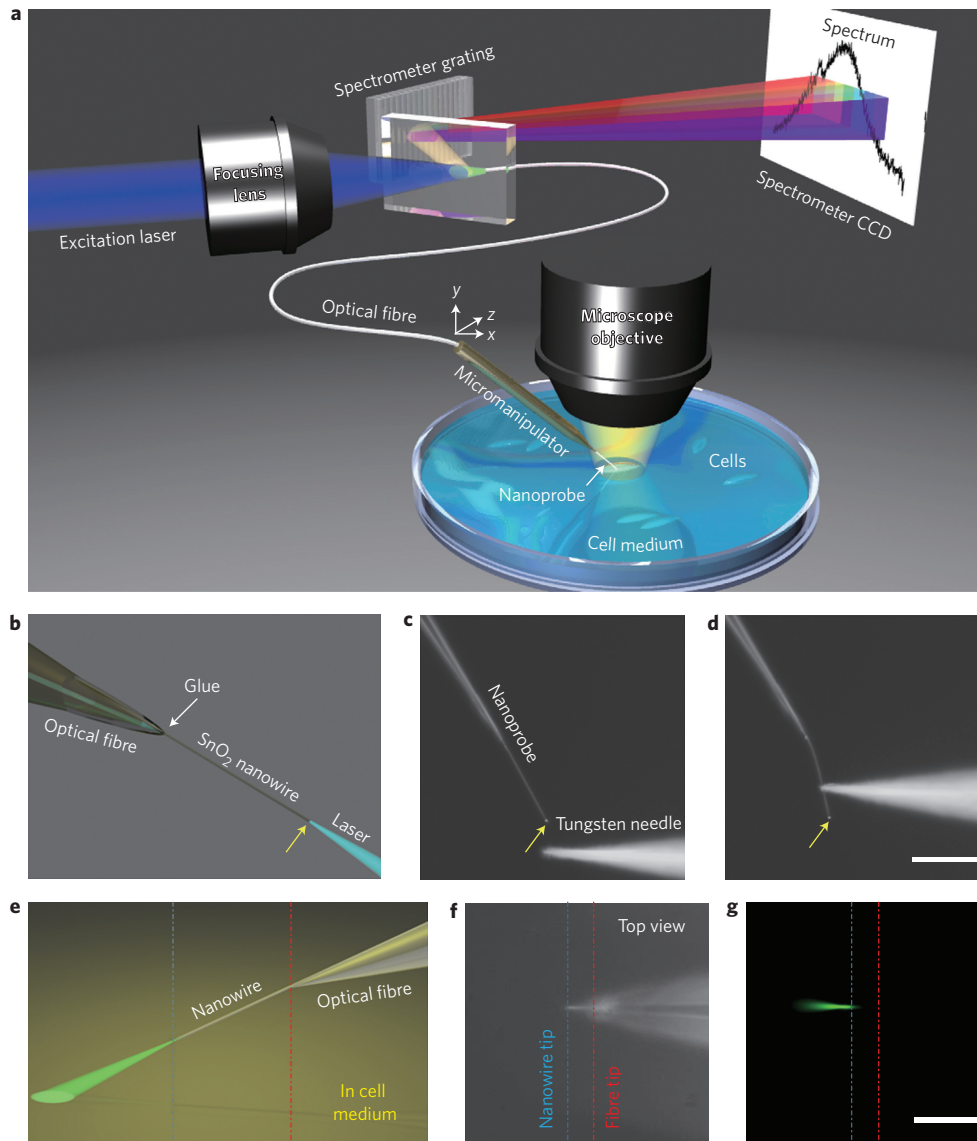


**Figure 1 | Design of the nanowire-based optical probe for single-cell endoscopy.** **a**, Schematic illustration of the nanowire-based cell endoscope system. The nanowire endoscope, consisting of a nanowire waveguide fixed on the tapered tip of an optical fibre, can be inserted into a single living cell at designated positions using a three-axis micromanipulating system for spot delivery of payloads. The nanowire endoscope can be optically coupled to either an excitation laser to function as a local light source for subcellular imaging or a spectrometer to collect local optical signals. CCD, charge-coupled device. **b**, Three-dimensional schematic showing a blue laser waveguided through a nanowire endoscope constructed by gluing a  $\text{SnO}_2$  nanowire to the tip of a tapered single-mode optical fibre. **c,d**, Dark-field images of an endoscope (coupled to a 442 nm blue laser) before (**c**) and during (**d**) deformation by a tungsten needle, showing that the nanowire endoscope is flexible and robust. Yellow arrows in **b–d** point to the nanowire tip where the waveguided light was emitted into free space. **e–g**, Intensity profile of the nanowire endoscope emission. Schematic drawing (**e**), dark-field (**f**) and fluorescence (**g**) images of a nanowire endoscope immersed in cell culture medium, which illuminated fluorescent proteins with blue light emitted from the nanowire tip. **f** and **g** are top views of the real nanowire endoscope device illustrated in **e**. A 442 nm long-pass filter was applied to remove the excitation beam from the fluorescence image (**g**). Scale bars, 50  $\mu\text{m}$ .

death (Supplementary Table S1, Fig. S5), apoptosis (Supplementary Fig. S6), significant cellular stress (Supplementary Fig. S7, Video S2) or membrane rupture (Supplementary Fig. S8) under the experimental conditions required for the spot cargo delivery and endoscopy studies described below. In contrast, insertion of a tapered optical-fibre tip caused 40% of the plated cells to die, and also induced considerable cellular stress and cell membrane rupture (Supplementary Section II). Moreover, illuminating the intracellular environment of HeLa cells with blue light using the nanoprobe did not harm the cells, because the illumination volume was small (down to the picolitre scale; Supplementary Table S2).

Having shown that the nanowires are biocompatible, we used the endoscopes to deliver payloads into specific sites in the cell. Carbon and boron nitride nanotube-based delivery systems have been reported previously<sup>1,28</sup>, in which the payloads (for example, quantum dots, QDs) were attached to the nanotube by disulphide bond linkers, which are cleavable in the reducing environment of the cytoplasm. A major limitation of this passive delivery system is the long insertion time (20–30 min) and the lack of temporal control over the delivery process (Supplementary Fig. S9). To reduce insertion time and improve temporal control during delivery, we attached QDs to the nanowire tip by means of photo-cleavable linkers (Fig. 2a–c) that

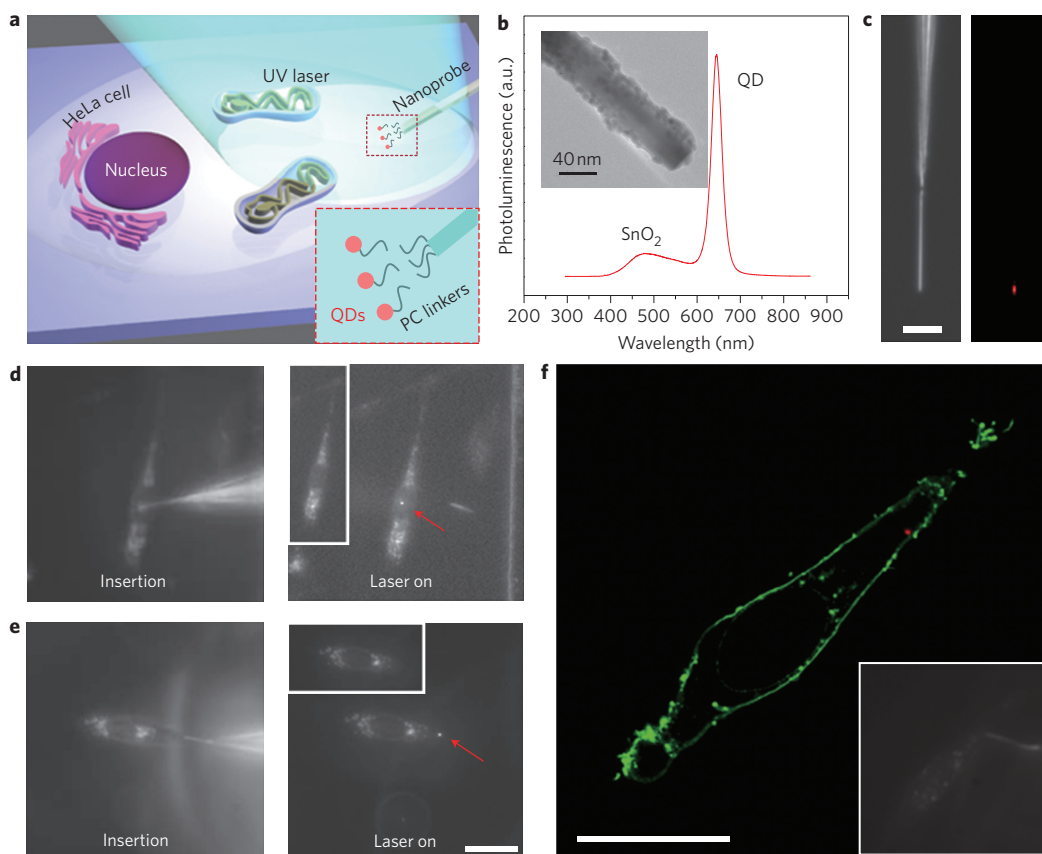


**Figure 2 | Spatiotemporal delivery of QDs into a single living HeLa cell.** **a**, Schematic of the spatiotemporal delivery of QDs into a living cell using a photoactivatable nanowire endoscope. Inset: QDs were conjugated to the nanowire by photocleavable (PC) linkers. **b**, Photoluminescence spectrum of a QD (emission, 655 nm)-conjugated  $\text{SnO}_2$  nanowire endoscope excited with a focused HeCd laser (325 nm). Inset: transmission electron microscope (TEM) image of the QD-conjugated  $\text{SnO}_2$  nanowire endoscope. Nanowires with smaller sizes than the average nanowire endoscopes had better contrast and were selected for TEM imaging. **c**, Dark-field (left) and fluorescence (right) images of the QD-conjugated  $\text{SnO}_2$  nanowire endoscope. **d,e**, Dark-field images showing a nanowire endoscope inserted into a cell nucleus (**d**, left) and cytoplasm (**e**, left), and fluorescence images taken after UV irradiation (325 nm, 1 min) was focused on the nanowire tip, showing QD fluorescence in the cell nucleus region (**d**, right) and in the cell cytoplasm (**e**, right) under 442 nm laser excitation. Dark-field illumination was left on when the fluorescence image was captured to show the cell outline. Insets in **d** and **e**: dark-field images of the two cells when the 442 nm excitation laser was turned off. A 532 nm long-pass filter was used to screen the excitation laser for the fluorescence imaging. Magnifications for **d** and **e** are the same. **f**, Fluorescence confocal image of a HeLa cell, showing that the nanowire has delivered the QDs (red dot in the cytoplasm) within the cell membrane (green), which was labelled with an Alexa Fluor 488 conjugate of WGA. A 488 nm laser was used to excite both the cell membrane stain and the QDs. Inset: dark-field image of the cell during QD delivery with a nanowire endoscope. Scale bars in **c,e,f**, 20  $\mu\text{m}$ .

can be cleaved by low-power ultraviolet radiation. Following insertion into the cell and within 1 min of illumination by ultraviolet laser, the functionalized endoscope released the QDs into the intended intracellular sites (Fig. 2d,e). Confocal microscopy scanning of the cell showed that the QDs were located within the cytoplasm, bordered by the fluorescently labelled membrane, confirming that QDs were successfully delivered (Fig. 2f). Photoactivation at this level had no significant effect on cell viability (Supplementary Table S2). The QD delivery set-up could be further integrated by fabricating the nanowire endoscope with an ultraviolet transparent optical fibre, so that the required ultraviolet excitation can be delivered directly through the nanowire.

The nanowire endoscope illumination is capable of high-resolution and high-contrast subcellular imaging and tracking of fluorescent species (Fig. 3a). The illumination resolution was first studied with QDs because they have high fluorescence efficiency in cellular environments. A highly directional laser beam from the nanowire could selectively illuminate one of two QD clusters located 2  $\mu\text{m}$  apart (Fig. 3b,c). Intracellular fluorescent molecules, which are far less bright than QDs, can also be locally excited (Fig. 3d–f; Supplementary Fig. S12–S14). Because of the small illumination area (down to a picolitre scale) and the small separation

that can be achieved between the light source and the fluorescent molecules, the endoscope illumination also ensures low background fluorescence and high imaging contrast. Figure 3d shows the fluorescence image of a HeLa cell stained with a fluorescent label that binds specifically to the cell membrane. Under such wide-field illumination, which is typical of epifluorescence microscopy, the whole cell membrane, both the top and bottom surfaces, was excited due to the large illumination depth. As a result, out-of-focus fluorescence can enter the focal plane of the objective and obscure the details of the in-focus image<sup>29</sup>. With its much smaller illumination depth, the nanowire endoscope can excite tiny areas on the cellular membrane with much lower background. Figure 3e,f demonstrates the spot illumination capability when the nanowire approached the cell membrane from the side, and Supplementary Fig. S14 further shows that it is possible to distinguish the fluorescence signals from the top and bottom of the cell membrane with the highly localized endoscope illumination. Furthermore, the high-spatial-resolution imaging capability of the nanowire endoscope was not achieved by sacrificing its temporal resolution. The nanowire endoscope can also be used for subcellular fluorescence tracking (Supplementary Fig. S15) and is potentially useful for sensing molecular kinetics in intracellular substructures (such as mitochondria).

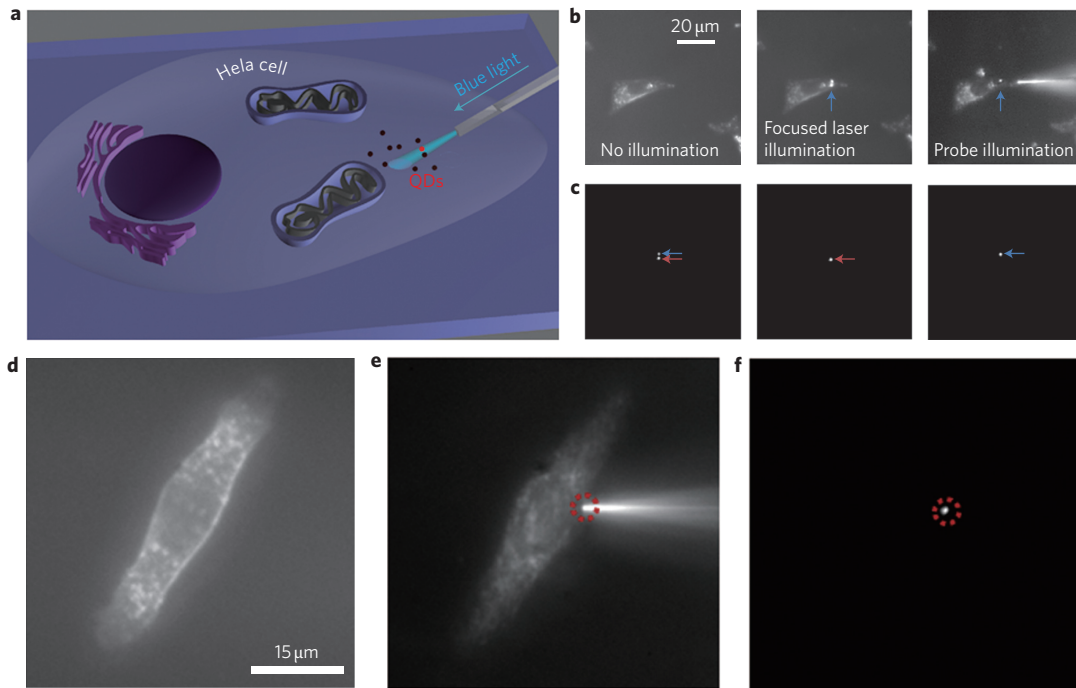


**Figure 3 | Subcellular imaging with nanowire endoscopes in a single living cell.** **a**, Schematic of the subcellular imaging of QDs in a living cell using a nanowire endoscope. **b**, Dark-field (left) and QD fluorescence (middle and right) images showing the imaging of two adjacent clusters of QDs ( $\sim 2 \mu\text{m}$  apart) using a focused 442 nm HeCd laser (middle) and endoscope illumination (right) with the same laser waveguided through the probe. In the middle and left panels, the dark-field illumination was left on to show the outline of the cell. Each cluster of QDs was delivered into the cell using the photoactive nanowire endoscope as described in Fig. 2. **c**, Fluorescence images of the QDs in **b** showing the spatial resolution of the local illumination by the nanowire endoscope. **d**, Fluorescence image of a live HeLa cell, labelled with a cell membrane stain, the Alexa Fluor 488 conjugate of WGA, illuminated by wide-field 442 nm excitation. **e, f**, Dark-field (**e**) and fluorescence (**f**) images of the cell shown in **d**, illuminated by a nanowire endoscope ( $\lambda = 442 \text{ nm}$ ).

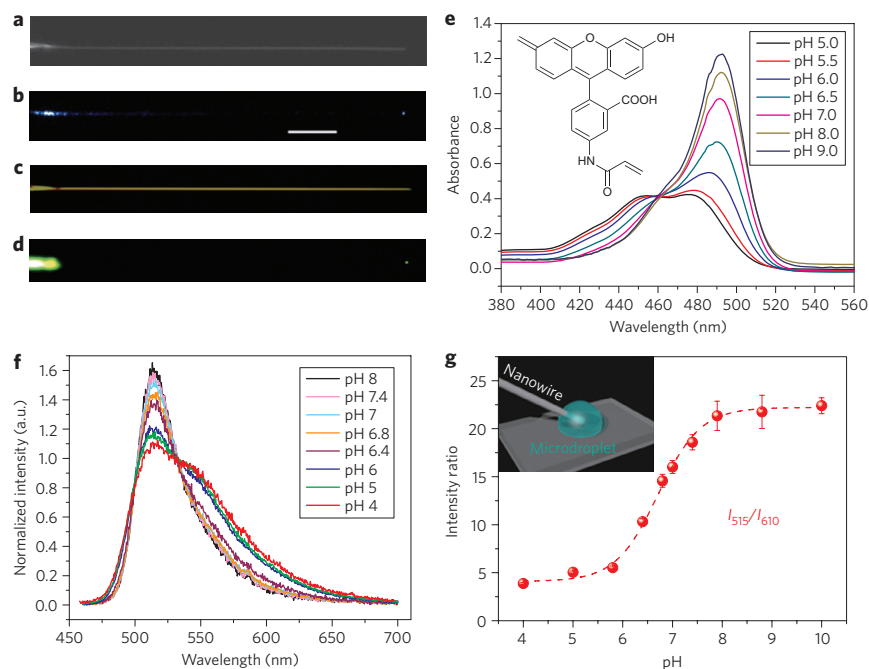


**Figure 4 | Local sensing of pH by the nanowire endoscope.** **a**, Dark-field image of a nanowire endoscope before coating with pH-sensitive fluorescent polymer. **b**, Colour digital image of blue laser (442 nm) waveguided through the nanowire endoscope. **c**, Dark-field image of the nanowire endoscope after polymer coating. **d**, Colour digital images showing the fluorescence of the nanowire coated with pH-sensitive fluorescent polymer after blue light is waveguided through it. Scale bar,  $5 \mu\text{m}$ . **e**, UV-vis absorption spectra of pH-sensitive dye (N-fluorescein acrylamide, FLAC) in buffer solutions of different pH. Inset: molecular structure of FLAC in its protonated form. **f**, Normalized probe tip fluorescence spectra in buffer solutions of different pH. **g**, Calibration curve of the dye-coated nanowire endoscope in a microdroplet containing buffer solution at different pH. Inset: schematic showing the measurement set-up with the nanowire tip immersed in the microdroplet of buffer solution.

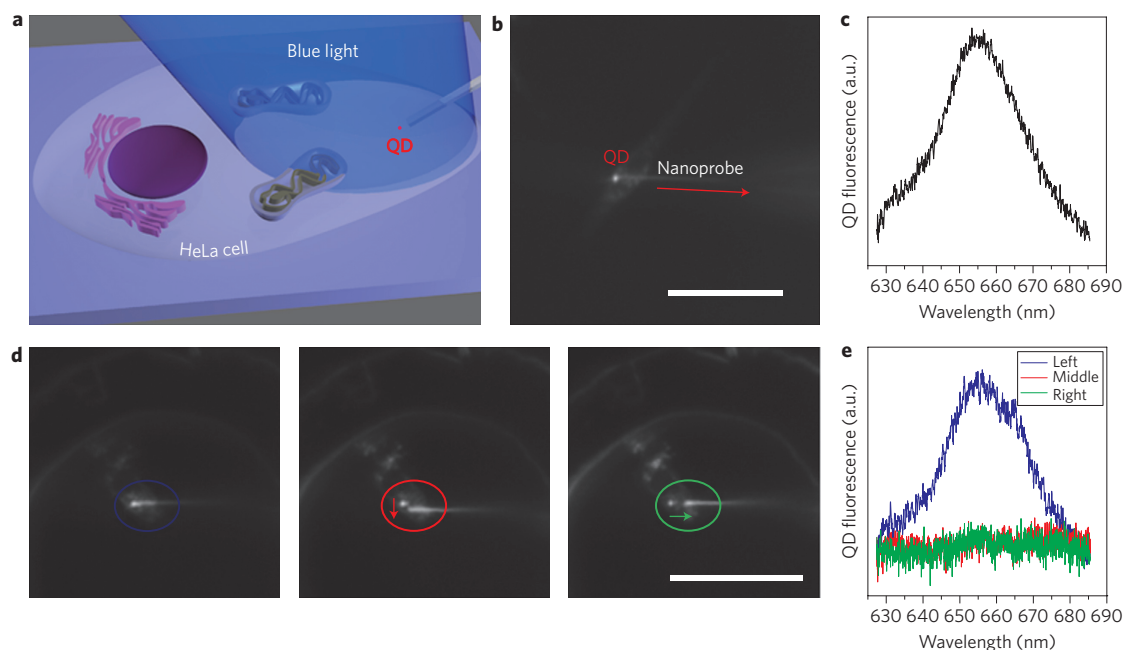


**Figure 5 | Near-field collection of QD fluorescence in a single living HeLa cell.** **a**, Schematic of the local detection of QD fluorescence in a living cell using a nanowire endoscope. The endoscope was placed near the QD ( $\lambda_{em} = 655$  nm), which was pre-loaded in the cytoplasm and excited by a blue laser beam. QD fluorescence was collected locally through the nanowire endoscope, which was coupled to a spectrometer. **b**, Dark-field/fluorescence image of a nanowire endoscope placed close to a QD cluster in the cytoplasm that was excited by a focused laser beam (442 nm). **c**, Spectrum of QD fluorescence collected through the endoscope, showing a single peak centred at  $\sim 655$  nm. **d**, Dark-field/fluorescence images of a nanowire endoscope in close contact with a QD cluster in a HeLa cell (left), and separated vertically by  $2 \mu\text{m}$  (middle) and horizontally by  $6 \mu\text{m}$  (right) from the QD cluster. Coloured circles mark the position of the QD cluster and the tip of the nanowire. Coloured arrows in the middle and right panels indicate the endoscope movement with respect to its position in the left panel. **e**, Spectra of QD fluorescence collected through the endoscope corresponding to the three images in **d**, respectively. The QD signal faded quickly as the endoscope was moved away from the QD cluster. A 532 nm long-pass filter was used to screen the excitation laser for fluorescence imaging. Scale bars,  $50 \mu\text{m}$ .

A pH-sensitive endoscope was also fabricated by coating the nanowire tip with a polymer embedded with pH-sensitive dyes (Fig. 4a–e). Preliminary tests showed that the functionalized nanowire endoscope can sense a change in pH in a submicrometre environment. The tip of the pH-sensitive endoscope, when immersed into microdroplets ( $<10$  pl in volume) of buffer solutions of different pH values, was able to report pH-dependent fluorescence from the endoscope tip. A calibration curve with a sharp transition between pH 5 and 9 was established (Fig. 4f,g).

As well as illumination from the tip of the nanowire endoscope, we also showed that fluorescence signals from subcellular regions can be collected through the endoscope. As illustrated in Fig. 5a–c, the fluorescence spectra of a single QD cluster in the cytoplasm was collected by the tip of a nanowire endoscope placed next to the cluster. Signal collection was very sensitive to the distance between the QD cluster and the nanowire tip (Fig. 5d,e), opening up the possibility for high-spatial-resolution fluorescence mapping and probing of the interior of non-transparent living biological objects, which would be impossible for bulky near-field scanning optical microscope tips.

In conclusion, we have developed a versatile and biocompatible nanowire-based optical probe for intracellular cargo delivery with high spatiotemporal precision and endoscopy with high spatial and temporal resolution. These nanowire endoscopes are highly flexible and robust, both mechanically and optically, and can endure repeated bending and deformation during a cell-imaging process. The effective optical coupling between the fibre-optics and the nanowire enables highly localized excitation and detection, limiting the probe volume close to the nanowire. The endoscope is a promising candidate for high-resolution optical imaging, mapping and chemical/biological sensing, as well as for precision delivery of gene, proteins and drugs.

## Methods

**SnO<sub>2</sub> nanowire synthesis.** This experimental procedure is described in the Supplementary Information.

**Optical-fibre etching.** This experimental procedure is described in the Supplementary Information.

**Nanowire endoscope fabrication.** The fabrication procedure of the nanowire endoscope is illustrated by the schematics in Supplementary Fig. S1. First, a SnO<sub>2</sub> nanowire (100–250 nm) was picked up from the substrate with a motorized three-axis micromanipulator (spatial resolution, 100 nm per step) and put on top of the tapered tip of a chemically etched single-mode optical fibre with a cone angle of  $3\text{--}5^\circ$  and tip diameter of 300–500 nm (S405-HP and 630-HP, Thorlabs). The relative position of the nanowire and fibre tip was adjusted to minimize the scattering loss at the nanowire–fibre junction. A droplet of premixed epoxy glue (ITW Devcon) or polydimethylsiloxane (Sylgard 184 Silicone Elastomer, Dow-Corning) was then applied to the overlapping nanowire–fibre junction with the micromanipulator needle to bond them permanently.

**QD conjugation onto the SnO<sub>2</sub> nanowire.** This experimental procedure is described in the Supplementary Information.

**Optical set-up.** All experiments reported in this work were performed on an upright dark-field optical microscope (Nikon). A HeCd laser (Melles Griot) supplied unpolarized continuous-wave (c.w.) ultraviolet excitation (325 nm) to the photo-cleavable linkers and 442 nm visible excitation for QD fluorescence. The lasers were focused either directly on the cell at a  $\sim 20^\circ$  glancing angle with the focal plane of the microscope objective lens, or on the tip of the optical fibre mounted on a five-axis single-mode optical-fibre coupler (Newport Corporation). A 650 nm c.w. diode laser (Thorlabs) was used to test the nanowire endoscope coupling for 630HP fibres. Dark-field and fluorescence images were collected through  $\times 20$  (NA = 0.40) and  $\times 50$  (NA = 0.55) long-working-distance objectives and recorded with a microscope-mounted camera (iXon, Andor Technology). Spectra were acquired by connecting the optical fibre to a UV-vis spectrometer (gratings at  $1,200$  grooves  $\text{mm}^{-1}$ , SpectraPro 300i, Roper Scientific) and a liquid-nitrogen-cooled charge-coupled device set-up. A 532 nm long-pass filter was always used for fluorescence imaging.

**Payload delivery experiment.** HeLa cells were seeded into a 35 mm Petri dish with grids and cultured overnight (22,000 cells per dish) at  $37^\circ\text{C}$  in the presence of 10%

fetal bovine serum (FBS). The QD-conjugated photoactive nanowire endoscope mounted on the micromanipulator was slowly inserted into the nucleus or cytoplasm. The insertion region was immediately irradiated with the focused 325 nm HeCd laser at 0.4 mW cm<sup>-2</sup> for 1 min, then the probe was removed from the cell. The fluorescence of QDs translocated into the cell was imaged under 442 nm laser excitation. For confocal imaging, HeLa cells were seeded into a 35 mm glass-bottom Petri dish with grids, following the same procedure mentioned above. Cells were randomly chosen from the grid-cell culture dish for light-activated QD delivery with the nanowire endoscope, and the positions of the cells operated on were documented for relocation. Cells were then fixed with 4% paraformaldehyde, stained with an Alexa Fluor 488 conjugate of wheat germ agglutinin (WGA, Invitrogen) and kept in Hank's Balanced Salt Solution (HBSS) for imaging. Confocal image was collected with a Zeiss 710 inverted laser scanning confocal microscope with a ×40 oil-immersed objective and 488 nm laser excitation.

**Subcellular imaging experiment.** HeLa cells were seeded into a 35 mm Petri dish with grids and cultured overnight (22,000 cells per dish) at 37 °C in the presence of 10% FBS. For subcellular QD imaging, two QD clusters were pre-delivered to adjacent spots (~2 μm apart) in the cytoplasm with photoactive nanowire endoscopes. An unmodified nanowire endoscope was placed close to the two QD clusters without direct contact with the cell membrane. The nanowire endoscope was mounted on the micromanipulator to offer precision control over the nanowire endoscope position. The distal end of the optical fibre was coupled to a 442 nm blue HeCd laser with an input power of 0.4 mW through a single-mode fibre coupler. For cell membrane illumination, HeLa cells were pre-treated with an Alexa Fluor 488 conjugate of WGA and kept in HBSS for imaging.

**Local collection experiment.** HeLa cells were seeded into a 35 mm Petri dish with grids and cultured overnight (22,000 cells per dish) at 37 °C in the presence of 10% FBS. The cells were pre-treated with aminated QDs for 1 h and rinsed several times with PBS. QD fluorescence was excited by a focused 442 nm blue laser. The nanowire endoscope was placed close to the QDs in the cytoplasm to pick up the local fluorescence signal. The distal end of the optical fibre was connected to a UV-vis spectrometer and the gratings were calibrated with 442 nm and 650 nm laser lines. The location of the nanowire endoscope was precisely controlled using the micromanipulator during the experiment.

Received 30 August 2011; accepted 18 November 2011;  
published online 18 December 2011

## References

- Chen, X., Kis, A., Zettl, A. & Bertozzi, C. R. A cell nanoinjector based on carbon nanotubes. *Proc. Natl Acad. Sci. USA* **104**, 8218–8222 (2007).
- Han, S. W. *et al.* A molecular delivery system by using AFM and nanoneedle. *Biosens. Bioelectron.* **20**, 2120–2125 (2005).
- Han, S. W. *et al.* Gene expression using an ultrathin needle enabling accurate displacement and low invasiveness. *Biochem. Biophys. Res. Commun.* **332**, 633–639 (2005).
- Yum, K., Wang, N. & Yu, M. F. Electrochemically controlled deconjugation and delivery of single quantum dots into the nucleus of living cells. *Small* **6**, 2109–2113 (2010).
- Yum, K. *et al.* Mechanochemical delivery and dynamic tracking of fluorescent quantum dots in the cytoplasm and nucleus of living cells. *Nano. Lett.* **9**, 2193–2198 (2009).
- Singhal, R. *et al.* Multifunctional carbon-nanotube cellular endoscopes. *Nature Nanotech.* **6**, 57–64 (2011).
- Cai, D. *et al.* Highly efficient molecular delivery into mammalian cells using carbon nanotube spearing. *Nature Methods* **2**, 449–454 (2005).
- Shalek, A. K. *et al.* Vertical silicon nanowires as a universal platform for delivering biomolecules into living cells. *Proc. Natl Acad. Sci. USA* **107**, 1870–1875 (2010).
- Niu, J. J., Schrlau, M. G., Friedman, G. & Gogotsi, Y. Carbon nanotube-tipped endoscope for *in situ* intracellular surface-enhanced Raman spectroscopy. *Small* **7**, 540–545 (2011).
- Schrlau, M. G., Dun, N. J. & Bau, H. H. Cell electrophysiology with carbon nanopipettes. *ACS Nano* **3**, 563–568 (2009).
- Hell, S. W. Far-field optical nanoscopy. *Science* **316**, 1153–1158 (2007).
- Egging, C. *et al.* Direct observation of the nanoscale dynamics of membrane lipids in a living cell. *Nature* **457**, 1159–1162 (2009).
- Zhuang, X. Nano-imaging with STORM. *Nature Photon.* **3**, 365–367 (2009).
- Tan, W. *et al.* Submicrometer intracellular chemical optical fiber sensors. *Science* **258**, 778–781 (1992).
- Vo-Dinh, T., Alarie, J.-P., Cullum, B. M. & Griffin, G. D. Antibody-based nanoprobe for measurement of a fluorescent analyte in a single cell. *Nature Biotechnol.* **18**, 764–767 (2000).
- Kasili, P. M., Song, J. M. & Vo-Dinh, T. Optical sensor for the detection of Caspase-9 activity in a single cell. *J. Am. Chem. Soc.* **126**, 2799–2806 (2004).
- Vo-Dinh, T. & Kasili, P. Fiber-optic nanosensors for single-cell monitoring. *Anal. Bioanal. Chem.* **382**, 918–925 (2005).
- Flusberg, B. A. *et al.* Fiber-optic fluorescence imaging. *Nature Methods* **2**, 941–950 (2005).
- Wu, Y. I. *et al.* A genetically encoded photoactivatable Rac controls the motility of living cells. *Nature* **461**, 104–108 (2009).
- Andrasfalvy, B. K., Zemelman, B. V., Tang, J. Y. & Vaziri, A. Two-photon single-cell optogenetic control of neuronal activity by sculpted light. *Proc. Natl Acad. Sci. USA* **107**, 11981–11986 (2010).
- Lippincott-Schwartz, J. & Patterson, G. H. Development and use of fluorescent protein markers in living cells. *Science* **300**, 87–91 (2003).
- Bulina, M. E. *et al.* A genetically encoded photosensitizer. *Nature Biotechnol.* **24**, 95–99 (2006).
- Law, M. *et al.* Nanoribbon waveguides for subwavelength photonics integration. *Science* **305**, 1269–1273 (2004).
- Sirbul, D. J. *et al.* Optical routing and sensing with nanowire assemblies. *Proc. Natl Acad. Sci. USA* **102**, 7800–7805 (2005).
- Kim, W. *et al.* Interfacing silicon nanowires with mammalian cells. *J. Am. Chem. Soc.* **129**, 7228–7229 (2007).
- Hallstrom, W. *et al.* Gallium phosphide nanowires as a substrate for cultured neurons. *Nano. Lett.* **7**, 2960–2965 (2007).
- Shalek, A. K. *et al.* Vertical silicon nanowires as a universal platform for delivering biomolecules into living cells. *Proc. Natl Acad. Sci. USA* **107**, 1870–1875 (2010).
- Yum, K. *et al.* Mechanochemical delivery and dynamic tracking of fluorescent quantum dots in the cytoplasm and nucleus of living cells. *Nano. Lett.* **9**, 2193–2198 (2009).
- Conchello, J. A. & Lichtman, J. W. Optical sectioning microscopy. *Nature Methods* **2**, 920–931 (2005).
- Pan, Z. W., Dai, Z. R. & Wang, Z. L. Nanobelts of semiconducting oxides. *Science* **291**, 1947–1949 (2001).
- Haber, L. H., Schaller, R. D., Johnson, J. C. & Saykally, R. J. Shape control of near-field probes using dynamic meniscus etching. *J. Microsc.* **214**, 27–35 (2004).

## Acknowledgements

This work was supported by the National Institutes of Health (grant no. R21 EB007474-03) and Department of Energy (contract no. DE-AC02-05CH11231). The authors thank Z. Huo for transmission electron microscope observations, D. Sirbul for the nanowire endoscope bending video, H.E. Jeong, J.W. Lee and Q. Pan for cell culturing, and Q. Pan and S. Gweon for discussions. P.Y. thanks the National Science Foundation for the A. T. Waterman Award.

## Author contributions

R.Y., J.P., Y.C., L.P.L. and P.Y. conceived and designed the research. C.H., Y.C. and S.Y. prepared cell samples and performed the calcein live cell assay after cytotoxicity tests. R.Y., J.P. and Y.C. performed the experiments. R.X., J.P., Y.C., L.P.L. and P.Y. analysed the data. R.Y., J.P. and P.Y. wrote the manuscript.

## Additional information

The authors declare no competing financial interests. Supplementary information accompanies this paper at [www.nature.com/naturenanotechnology](http://www.nature.com/naturenanotechnology). Reprints and permission information is available online at <http://www.nature.com/reprints>. Correspondence and requests for materials should be addressed to P.Y.